

Mini Review

# Development of olefin metathesis catalyst precursors bearing nucleophilic carbene ligands

Laleh Jafarpour, Steven P. Nolan \*

Department of Chemistry, University of New Orleans, New Orleans, LA 70148-2820, USA

Received 19 June 2000; accepted 8 August 2000

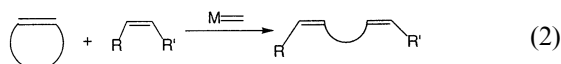
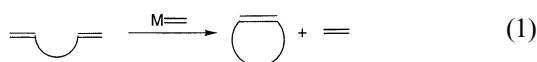
## Abstract

From solution calorimetric measurements involving binding of nucleophilic carbenes to a ruthenium centered organometallic system, steric and electronic properties of the carbenes were assessed. An understanding of these fundamental properties led to the development of novel olefin metathesis catalysts bearing these nucleophilic carbenes as ancillary ligands. The discovery and development of olefin metathesis active ruthenium catalysts bearing a nucleophilic carbene ancillary ligand are described. © 2001 Elsevier Science B.V. All rights reserved.

**Keywords:** Metathesis; Carbenes; Thermochemistry

## 1. Introduction

The last decade has witnessed the growing use of olefin metathesis in organic synthesis [1]. Ring closing metathesis (RCM, Eq. (1)) and ring opening metathesis (ROM, Eq. (2)) as well as combinations of these transformations have resulted in providing opportunities to build molecules of interest and importance.



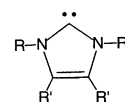
Two single-component, well-defined, metal-alkylidene compounds, the ruthenium alkylidene **1** developed by Grubbs [2] and the molybdenum alkylidene **2** developed in the Schrock laboratories [3] are the most widely used olefin metathesis initiators. Catalysts of the Grubbs type **1** (benzylidene and vinylalkylidene) are of special interest, since they are only moderately sensitive

to air and moisture and show significant tolerance of functional groups [2] (Fig. 1).

The ruthenium carbene complex,  $\text{RuCl}_2(\text{=C}(\text{H})\text{Ph})(\text{PCy}_3)_2$  (**3**), developed by Grubbs et al. is a highly efficient catalyst precursor and its use is widespread in organic and polymer chemistry [2,4]. This ruthenium complex has a distorted square-pyramidal structure with two *trans* chloride ligands and two *trans* phosphine ligands at the base of the pyramid with the carbene moiety at the apex. The catalytic activity of the



Fig. 1. Olefin metathesis catalysts.



R = alkyl, aryl, amine, ether

Fig. 2. Nucleophilic carbene.

\* Corresponding author. Tel.: +1-504-2866311; fax: +1-504-2806860.

E-mail address: snolan@uno.edu (S.P. Nolan).

Table 1

Enthalpies of ligand substitution, relative reaction enthalpy (kcal mol<sup>-1</sup>) and NMR data for the reaction: [Cp\*RuCl]<sub>4</sub> + 4L  $\xrightarrow[30^{\circ}\text{C}]{\text{THF}}$  4Cp\*Ru(L)Cl

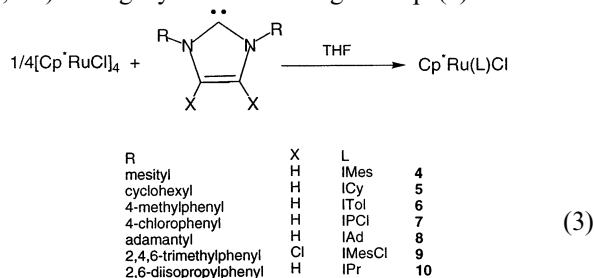
Complex	L	−Δ <i>H</i> <sub>rxn</sub> (kcal mol <sup>-1</sup> ) <sup>a</sup>	Relative BDE (kcal mol <sup>-1</sup> )	δ <sup>1</sup> H (Cp*) (400 MHz, 25°C, <i>d</i> <sub>8</sub> -THF)
<b>4</b>	IMes	62.6(0.2)	15.6	1.07
<b>5</b>	ICy	85.0(0.2)	21.2	1.67
<b>6</b>	ITol	75.3(0.4)	18.8	0.99
<b>7</b>	IPCl	74.3(0.3)	18.6	1.03
<b>8</b>	IAd	27.4(0.4)	6.8	1.49
<b>9</b>	IMesCl	48.5(0.4)	12.1	1.06
<b>10</b>	IPr	44.5(0.4)	11.1	1.20 <sup>b</sup>
<b>11</b>	PCy <sub>3</sub>	41.9(0.2)	10.5	1.48 <sup>b</sup>
<b>12</b>	P <sup><i>t</i></sup> Pr <sub>3</sub>	37.4(0.3)	9.4	1.43 <sup>b</sup>

<sup>a</sup> Enthalpy values are reported with 95% confidence limits<sup>b</sup> In C<sub>6</sub>D<sub>6</sub>.

complex originates from the liberation of one phosphine followed by coordination of the olefin substrate [2c]. The nature of the carbene moiety has been shown to influence not only the initiation but also the propagation of the catalytic reaction [2b]. Sterically demanding and highly donating phosphine ligands (PCy<sub>3</sub>) stabilize the intermediate catalytic species. Despite its versatility, this catalyst displays a low thermal stability as a result of easily accessible bimolecular decomposition pathways [5].

Nucleophilic carbene ligands imidazol-2-ylidenes are neutral, two-electron donor ligands with negligible π-back-bonding tendency. As such they can be viewed as alternatives to or mimics of phosphine ligands [6] (Fig. 2).

In view of this similarity and our longstanding interest in metal–phosphine thermochemistry, we conducted thermochemical and structural studies to determine the binding strength and the bulkiness of these carbenes [7]. Tilley and co-workers have reported the isolation of coordinatively unsaturated complexes Cp\*Ru(L)Cl (L = PCy<sub>3</sub> and P<sup>*t*</sup>Pr<sub>3</sub>) by a simple reaction with the tetrameric species [Cp\*RuCl]<sub>4</sub> [Cp\* = η<sup>5</sup>-C<sub>5</sub>Me<sub>5</sub>] [8]. This versatile starting material reacts rapidly with sterically demanding phosphines (PCy<sub>3</sub> and P<sup>*t*</sup>Pr<sub>3</sub>) as well as with the nucleophilic carbene ligands (L) to give deep blue, coordinatively unsaturated Cp\*Ru(L)Cl complexes **4–10** (L = 1,3-bis(2,4,6-trimethylphenyl) (IMes, **4**); 1,3-R<sub>2</sub>-imidazol-2-ylidene (R = cyclohexyl (ICy, **5**); 4-methylphenyl (ITol, **6**); 4-chlorophenyl (IPCl, **7**); adamantyl (IAd, **8**); 4,5-dichloro-1,3-bis(2,4,6-trimethylphenyl) (IMesCl, **9**) and 1,3-bis(2,6-diisopropylphenyl)imidazol-2-ylidene (IPr, **10**) in high yields according to Eq. (3).



## 2. Calorimetric studies

The reactions depicted in Eq. (3) are suitable for calorimetric investigations since they proceed rapidly and quantitatively as monitored by NMR spectroscopy. The solution calorimetric protocol has been described elsewhere [9]. The enthalpy values were determined by anaerobic solution calorimetry in THF at 30°C by reacting four equivalents of each carbene with one equivalent of [Cp\*RuCl]<sub>4</sub>. The results of this study are presented in Table 1.

The enthalpies of reaction can be converted into relative enthalpies of reaction on a mole of product basis by dividing the enthalpies by four (which represents the number of bonds made in the course of reaction). The difference between two relative enthalpy values in Table 1 represents the enthalpic driving force for a substitution between any two ligands listed. With the exception of IAd (**8**), all reactions involving carbene ligands show more exothermic reaction enthalpy values than PCy<sub>3</sub> and P<sup>*t*</sup>Pr<sub>3</sub>. From the relative enthalpy data, it is apparent that Cp\*Ru(PCy<sub>3</sub>)Cl should undergo a substitution of the phosphine ligand by a nucleophilic carbene.

## 3. Structural studies

The magnitude of the reaction enthalpies measured involving nucleophilic carbenes are influenced by the stereoelectronic properties of the ligands [6d]. An example of electronic influence is the 3.5 kcal mol<sup>-1</sup> enthalpy difference between the isosteric IMes and IMesCl ligands that shows the electron-withdrawing nature of Cl compared to H. This trend is in line with electron donor/withdrawing ability of arene substituents. The effect in this last case is a long-range electronic influence and is relatively small this presumably due to the distance separating the aryl and the carbene lone pair. Substituting an alkyl for an aryl group increases the donor ability of the carbene ligand. The case in point is the ICy that is some 5.6 kcal mol<sup>-1</sup> more exothermic than IMes. The

other alkyl-substituted carbene investigated is the adamantyl derivative IAd that is the least exothermic ligand examined. Steric effects are at the origin of this small enthalpy of ligand substitution involving IAd. Increase in steric congestion around the carbene carbon atom hinders a closer approach of the ligand, therefore affording smaller metal-carbene lone pair overlap. The calorimetric results offer a clear picture of the electronic

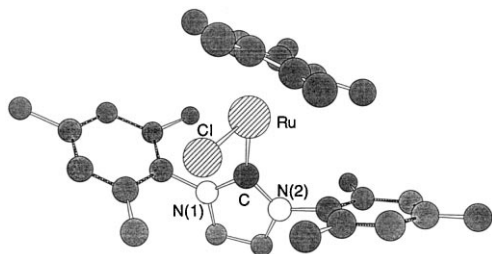


Fig. 3. Molecular structure of  $\text{Cp}^*\text{Ru}(\text{IMes})\text{Cl}$  (**4**). Hydrogen atoms are omitted for clarity.

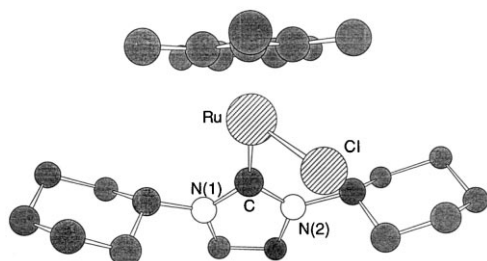


Fig. 4. Molecular structure of  $\text{Cp}^*\text{Ru}(\text{ICy})\text{Cl}$  (**5**). Hydrogen atoms are omitted for clarity.

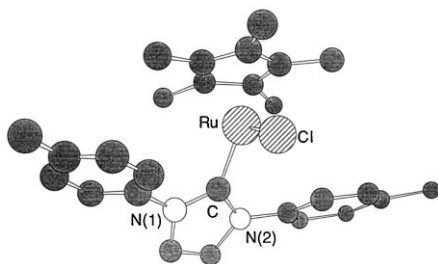


Fig. 5. Molecular structure of  $\text{Cp}^*\text{Ru}(\text{ITol})\text{Cl}$  (**6**). Hydrogen atoms are omitted for clarity.

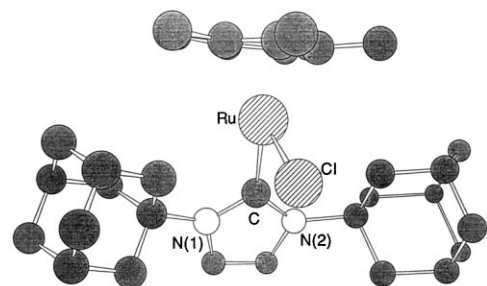


Fig. 6. Molecular structure of  $\text{Cp}^*\text{Ru}(\text{IAd})\text{Cl}$  (**8**). Hydrogen atoms are omitted for clarity.

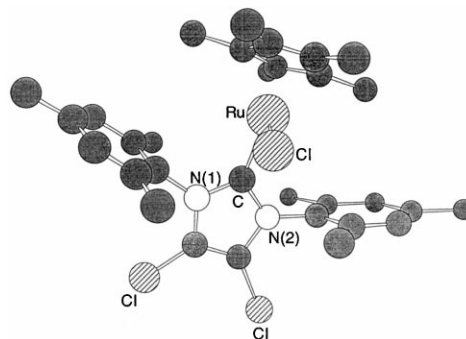


Fig. 7. Molecular structure of  $\text{Cp}^*\text{Ru}(\text{IMesCl})\text{Cl}$  (**9**). Hydrogen atoms are omitted for clarity.

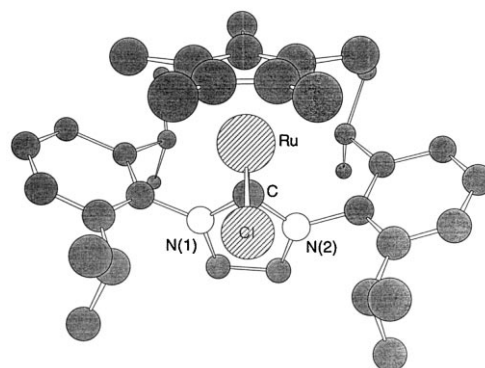


Fig. 8. Molecular structure of  $\text{Cp}^*\text{Ru}(\text{IPr})\text{Cl}$  (**10**). Hydrogen atoms are omitted for clarity.

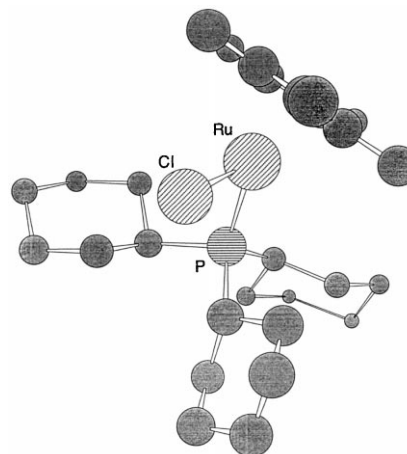


Fig. 9. Molecular structure of  $\text{Cp}^*\text{Ru}(\text{PCy}_3)\text{Cl}$  (**11**). Hydrogen atoms are omitted for clarity.

properties of the nucleophilic carbenes. To gauge the steric factors at play in the  $\text{Cp}^*\text{Ru}(\text{L})\text{Cl}$  system, structural studies were carried out on complexes **4** [10], **5** [7], **6** [7], **8** [7], **9** [10], **10** [11] and **11** [10] and were compared with structural data already available for  $\text{Cp}^*\text{Ru}(\text{P}^i\text{Pr}_3)\text{Cl}$  [8]. The structural models for complexes **4–6** and **8–11** are shown in Figs. 3–9 and a selection of bond angles and bond lengths is presented in Table 2.

Table 2

Carbene steric parameters ( $^{\circ}$ ) and selected bond lengths ( $\text{\AA}$ ) and angles ( $^{\circ}$ ) for complexes **4–6** and **8–12**

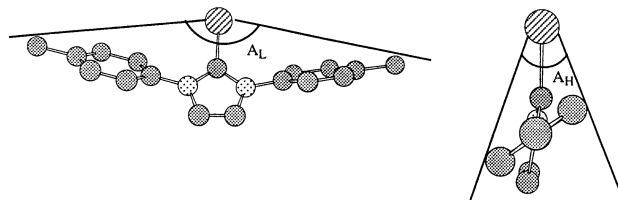
Complex	Carbene sterics ( $A_L$ and $A_H$ )	Ru–C	Ru–Cl	Ru–Cp*	C–Ru–Cl	C–Ru–Cp*	Cp*–Ru–Cl
<b>4</b>	150.7, 70.4	2.105	2.376	1.766	90.6	140.7	128.6
<b>5</b>	126.7, 31.8	2.070	2.524	1.658	93.7	129.3	15.5
<b>6</b>	155.2, 30.8	2.068	2.340	1.755	96.0	130.8	132.8
<b>8</b>	149.0, 41.4	2.153	2.438	1.778	87.9	138.7	130.4
<b>9</b>	152.0, 69.9	2.074	2.375	1.765	90.0	142.0	128.0
<b>10</b>	134.0, 137.6	2.086	2.371	1.754	89.32	141.5	129.2
<b>11</b>	115.8	2.383 <sup>a</sup>	2.378	1.771	91.2 <sup>a</sup>	138.9 <sup>a</sup>	129.9
<b>12</b>	100.8	2.395 <sup>a</sup>	2.365	1.810	91.4 <sup>a</sup>	139.2 <sup>a</sup>	129.3

<sup>a</sup> Replace C with P.

The variation of Ru–C(carbene) bond distances among ruthenium carbene complexes illustrates that nucleophilic carbene ligands are better donors when alkyl, versus aryl, groups are present. The exception, **8**, can be understood on the basis of large steric demands of the adamantyl groups on the imidazole framework which hinder the carbene lone pair availability. Comparison of the Ru–C(carbene) bond distances among the aryl substituted carbenes show that the least sterically encumbered carbene, ITol, has the shortest bond length. The difference in the aforementioned bond length between IMes and IMesCl results from the electronic effect of Cl imidazol-2-ylidene substituents. It should be noted that the enthalpy of reaction cannot be directly converted into an absolute bond disruption energy for the Ru–carbene in view of the existence of significant reorganization energies as depicted by variation in the Ru–Cp\* and Ru–Cl bond distances. A very clear example of the presence of this reorganization energy is evident when comparing the ICy and the ITol containing complexes **5** and **6**. Here, complex **5** is more stable than **6** by some 10 kcal mol<sup>-1</sup>, yet the Ru–C(carbene) distances are statistically identical. The largest difference between the two complexes resides in the differences in Ru–Cp\* centroid bond distance (a difference of 0.1  $\text{\AA}$  with **6** being longer than **5**) and the Ru–Cl bond distance (a difference of 0.18  $\text{\AA}$  with **5** being longer than **6**). When the aryl substituted carbene ruthenium complexes are examined, the Ru–C(carbene) versus enthalpy trend is evident and makes sense in terms of the electronic explanations discussed above. Here, there appears to be a small variation in the Ru–Cl and Ru–Cp\* bond distances from one complex to the other. Aryl- and alkyl-substituted carbenes behave differently. We propose that this difference in bonding behavior can be attributed to the presence of a  $\pi$  system in the aryl case which localizes (or contributes as an acceptor) the effect on the carbene ligand. This in turn diminishes the large reorganization effects present in the alkyl cases where a  $\pi$  system on the carbene substituent is absent. Additionally, the position of the Cp\* proton in the <sup>1</sup>H-NMR spectra of these complexes,

reported in Table 1, also supports this hypothesis. The aryl-substituted carbene complexes center around 1 ppm while the alkyl derivatives (including phosphines which are known as good donor ligands) are at ca. 1.5–1.7 ppm. The increased electron density on the Cp\* ring leading to greater shielding, affords shifts of the Cp\* resonance of higher frequency [12]. No straightforward bond strength/length correlation can be made in this system in view of the presence of the reorganization energy. It would be of use to quantify the steric factors characterizing this class of ligands. They cannot be viewed in the same light as phosphine ligands since a cone angle (as defined by Tolman [13]) cannot be defined in the present system. In terms of steric argument, the nucleophilic carbenes can be considered as ‘fences’, with ‘length’ and ‘height’. As a first model to describe these steric parameters, we propose two parameters that can be used to quantify the steric effect in this ligand class. These two quantities can be taken directly from the crystallographic data. The two views presented in Fig. 10 depict the method used to extract the two parameters.

Numerical values defining length and height of the carbene ‘fences’ are listed in Table 2. Not surprisingly, all aryl-substituted carbenes possess nearly the same large  $A_L$  value since the ‘length’ of the ligand is measured using the aryl para methyl group. The magnitude of the ‘height’ parameter ( $A_H$ ) depends on the presence or absence of ortho substituents. The most demanding aryl-substituted carbene ligand is the IMes ligand with 150.7 ( $A_L$ ) and 70.4 $^{\circ}$  ( $A_H$ ) as steric parameters. The alkyl substituted carbene ICy is the least sterically

Fig. 10. Determination of two steric parameters ( $A_L$  and  $A_H$ ) associated with carbene ligands in Cp\*Ru(L)Cl complexes.

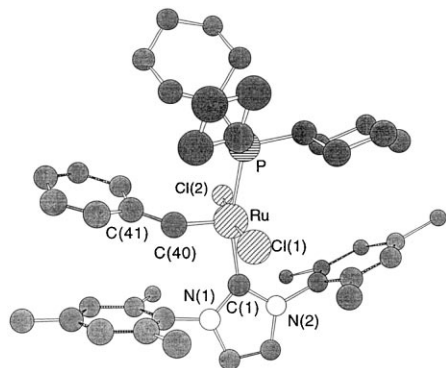


Fig. 11. Molecular structure of  $(\text{PCy}_3)\text{RuCl}_2(=\text{C}(\text{H})\text{Ph})(\text{IMes})$  (**13**). Hydrogen atoms are omitted for clarity.

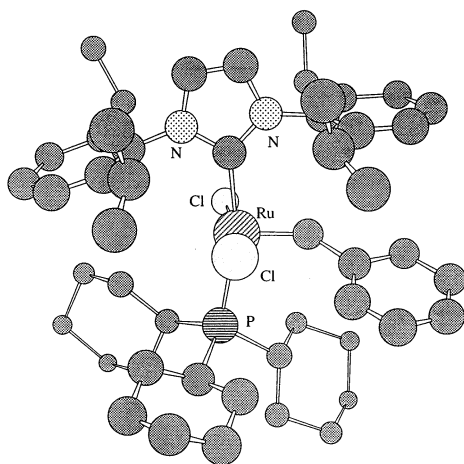


Fig. 12. Molecular structure of  $(\text{PCy}_3)\text{RuCl}_2(=\text{C}(\text{H})\text{Ph})(\text{IPr})$  (**14**). Hydrogen atoms are omitted for clarity.

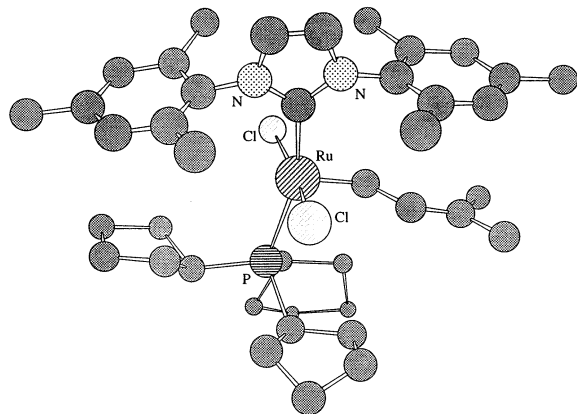


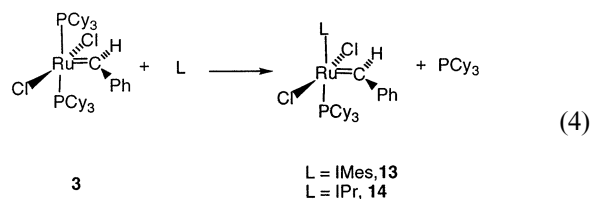
Fig. 13. Molecular structure of  $(\text{PCyp}_3)\text{RuCl}_2(=\text{CHCH}=\text{CMe}_2)(\text{IMes})$  (**15**). Hydrogen atoms are omitted for clarity.

demanding ligand investigated in the present series. The IAd ligand, although bearing sterically demanding adamantyl groups has an  $A_L$  parameter comparable to the aryl ligands examined and a smaller  $A_H$  parameter. The ICy ligand appears to be unique in the series

investigated. In complex **5**, the  $A_L$  angle is  $126.3^\circ$ . In the phosphine complexes **11** and **12** these angles were measured as  $115.8^\circ$  [8] and  $100.8^\circ$  [9]. The ICy is sterically more closely related to these two phosphine complexes.

#### 4. Ruthenium olefin metathesis-active complexes bearing a nucleophilic carbene ligand

We have shown that most of the substituted imidazol-2-ylidene studied form stronger covalent bonds to the ruthenium center than  $\text{PCy}_3$  (vide supra). Therefore, it might prove possible to replace one or both of the phosphine ligands in **3** with nucleophilic carbene ligands [14]. It has been noted that an increase in the ancillary phosphine electron donor ability leads to increased catalytic activity [15]. Since we have determined that the imidazol-2-ylidene carbenes such as IMes and IPr are better donors than  $\text{PCy}_3$ , the catalytic behavior should reflect this increased electron donor ability [10]. When both phosphines were replaced in **2** by imidazol-2-ylidene ligands they showed only little if any improvements in applications to ROMP and RCM [14a]. Upon using sufficiently bulky aryl imidazol-2-ylidene carbenes only one  $\text{PCy}_3$  is replaced (see Eq. (4)) [10,11,14c].



The structure of **13** and **14** were confirmed by single crystal X-ray diffraction study (see Figs. 11 and 12). The Ru–C (carbene) bond distances (1.841(11) and 1.817 Å for **13** and **14**, respectively) are the same as in  $\text{RuCl}_2(=\text{CH}-p\text{-C}_6\text{H}_4\text{Cl})(\text{PCy}_3)$ , (1.838(3) Å) [2b] and shorter than in  $\text{RuCl}_2(=\text{CHCH}=\text{CPh}_2)(\text{PCy}_3)_2$  (1.851(21) Å) [4a]. While two (formally) carbene fragments are present in **13** and **14**, they display different Ru–C distances (e.g. in **13** Ru–C(carbene), 1.841(11) and Ru–C(L), 2.069(11) Å). These important metrical parameters clearly distinguish two metal–carbene interactions: a covalently bound benzylidene and a datively bound imidazol-2-ylidene-carbene, the latter acting as a simple two-electron donor. From Figs. 11 and 12, it is also clear that the IMes and IPr ligands are sterically more demanding than  $\text{PCy}_3$ .

The exchange reaction of one phosphine ligand ( $\text{PCyp}_3$ , Cyp = cyclopentyl) in  $(\text{PCyp}_3)_2\text{RuCl}_2(=\text{CHCH}=\text{CMe}_2)$  with IMes results in the formation of  $\text{PCyp}_3\text{Ru}(\text{IMes})\text{Cl}_2(=\text{CHCH}=\text{CMe}_2)$  (**15**) [16]. A structure of **15** is presented in Fig. 13.

The metrical data for compounds **13** and **15** show similar bond distances and angles. The coordination

Table 3

Selected bond lengths (Å) and angles (°) for (PCy<sub>3</sub>)RuCl<sub>2</sub>(=C(H)Ph)(IMes) (**13**), (PCy<sub>3</sub>)RuCl<sub>2</sub>(=C(H)Ph)(IPr) (**14**), and (PCyp<sub>3</sub>)RuCl<sub>2</sub>(=CHCH=CMe<sub>2</sub>)(IMes) (**15**)

	Ru–C(L)	Ru–Cl(1, 2)	Ru–C (carbene)	Ru–P	C(carbene)– Ru–C(L)	C(carbene)– Ru–P	C(carbene)– Ru–Cl(1, 2)	P–Ru–Cl(1, 2)	C(L)–Ru– Cl(1, 2)
<b>13</b>	2.069(11)	2.393(3), 2.383(3)	1.841(11)	2.419(3)	99.2(5)	97.1(4)	104.3(5), 87.1(5)	89.51(10), 89.86(9)	90.4(3), 86.9(3)
<b>14</b>	2.088(2)	2.38.22(7), 2.4008(7)	1.817(3)	2.4454(7)	97.56(10)	96.64(8)	99.49(9), 88.87(9)	93.06(2), 90.59(2)	90.46(6), 83.77(6)
<b>15</b>	2.081(3)	2.4012(10), 2.3950(8)	1.764(4)	2.4487(10)	102.46(15)	95.55(13)	91.16(17), 97.37(17)	93.33(4), 87.28(4)	89.98(7), 86.75(7)

sphere around the metal center forms a distorted square pyramid with the benzylidene and vinylmethylene moiety at the apex. However, the distance of the apical carbene carbon to the metal center in **15** is shorter than that in **13**. Therefore, it can be inferred that the vinylmethylene moiety is more strongly bonded to ruthenium than the benzylidene. All other bond distances around the metal center are slightly longer in complex **15** than in complex **13**. The bulk of the fence created by the IMes ligand sterically interferes with the carbene moiety and causes the bond angles to undergo large deviations. Selected bond distances and bond angles are presented in Table 3.

The catalytic activity of these new complexes (**13** and **14** and **15**) was tested by using the standard ring closing metathesis (RCM) substrate, diethyldiallylmalonate (Scheme 4 reaction 1). Results are shown in Table 4 [10,11].

Moreover, the thermal stability of the imidazol-2-ylidene bearing complexes **13** and **14** and **15** were compared to those of **3** and (PCyp<sub>3</sub>)<sub>2</sub>RuCl<sub>2</sub>(=CHCH=CMe<sub>2</sub>). Results of these studies show that where the original phosphine bearing catalyst precursors **2** and (PCyp<sub>3</sub>)<sub>2</sub>RuCl<sub>2</sub>(=CHCH=CMe<sub>2</sub>) decompose within 1 and 2 h, respectively, at 60°C, **13**, **14** and **15** are more robust. In fact their decomposition starts after 2 weeks when heated at 60°C [10,11,16]. This early study showed that the imidazol-2-ylidene analogs of Grubbs systems could act as olefin metathesis catalyst precursors, displaying significant activity and improved thermal stability. An improved synthesis making use of a one-pot approach has recently appeared [17].

Grubbs et al. have prepared the saturated version of imidazol-2-ylidenes, 4,5-dihydroimidazol-2-ylidenes (Fig. 14) [18]. They proposed the higher basicity of the saturated imidazole ligand compared to its unsaturated analogues would translate into an increased reactivity of the desired catalysts. The ruthenium complexes formed (RuCl<sub>2</sub>(=C(H)Ph)(PCy<sub>3</sub>)(1,3-R<sub>2</sub>-4,5-dihydroimidazol-2-ylidene)) showed increased ring-closing metathesis activity compared to their phosphine analogues. Recent work indicates these nucleophilic car-

bene substituted ruthenium complexes are very active in cross metathesis of olefins [19].

### 5. (*p*-Cymene)RuLCl<sub>2</sub> (L = IMes and IPr) and related complexes as RCM catalysts

Recently, the possibility that complexes of unsaturated 'C<sub>α</sub>' ligands other than alkylidenes might also serve as catalyst precursors in olefin metathesis has received more attention [20]. For example, it has been shown that (*p*-cymene)RuCl<sub>2</sub>(PCy<sub>3</sub>) (**16**), and its cationic, 18-electron allenylidene derivative, [(*p*-cymene)RuC<sub>2</sub>(PCy<sub>3</sub>)(=C=C=CPh)]PF<sub>6</sub> (**17**), are active catalyst precursors for various ring closing metathesis (RCM) reactions [21]. In every example mentioned above the use of sterically demanding and electron donating phosphines is required to stabilize reactive intermediates. Hence, it was of interest to synthesize the imidazol-2-ylidene analogues of these complexes and test their catalytic activity in olefin metathesis. Reaction of commercially available [(*p*-cymene)RuCl<sub>2</sub>]<sub>2</sub> (**18**) with IMes or IPr in THF at room temperature results in the

Table 4

Ring closing metathesis of diallylmalonate using catalyst precursors **3**, **13**, **14**, and **15**

Catalyst precursor <sup>a</sup>	Temperature (°C)	Time (min)	Yield (%) <sup>b</sup>
<b>3</b>	RT	15	85
<b>13</b>	RT	15	92
<b>14</b>	RT	15	100
<b>15</b>	RT	15	10

<sup>a</sup> Catalyst precursor loading = 5 mol%.

<sup>b</sup> Calculated from <sup>1</sup>H-NMR spectra.

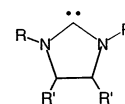


Fig. 14. 1,3-R<sub>2</sub>-4,5-dihydroimidazol-2-ylidene.

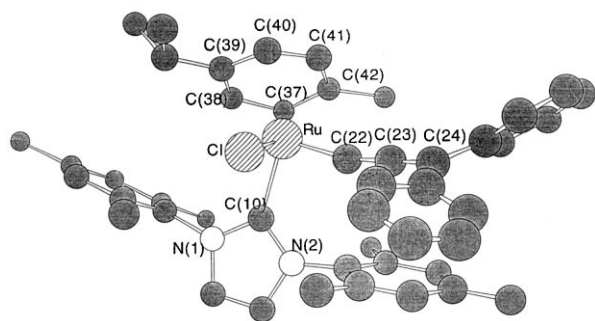
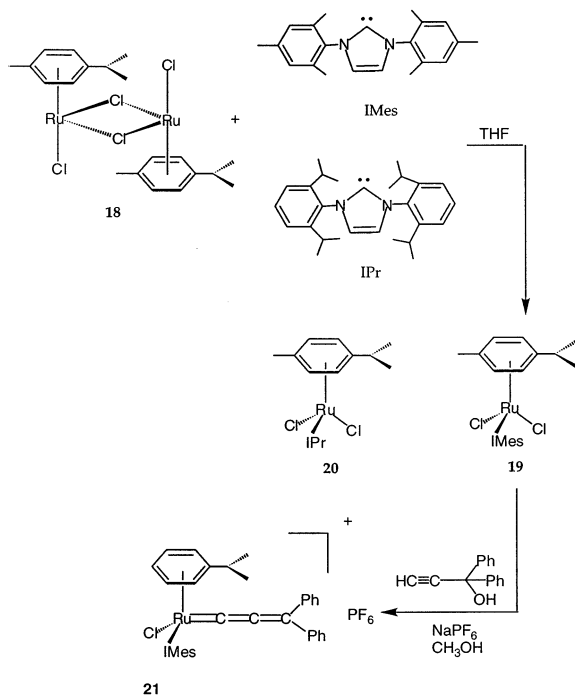


Fig. 15. Molecular structure of  $[(p\text{-cymene})\text{RuCl}(\text{IMes})(=\text{C}=\text{C}=\text{CPh}_2)]\text{PF}_6$  (**21**). Hydrogen atoms and  $\text{PF}_6^-$  anion have been omitted for clarity.

formation of  $(p\text{-cymene})\text{RuCl}_2(\text{IMes})$  (**19**) and  $(p\text{-cymene})\text{RuCl}_2(\text{IPr})$  (**20**) in good yields. Treating **19** with 1,1-diphenylprop-2-ynyl alcohol in the presence of  $\text{NaPF}_6$  results in the formation of  $[(p\text{-cymene})\text{RuCl}(\text{IMes})(=\text{C}=\text{C}=\text{CPh})]\text{PF}_6$  (**21**) (Scheme 1) [20e].

A structural model of **21** is shown in Fig. 15. The coordination geometry around the Ru center can be considered as a three-legged piano stool.  $p$ -Cymene is bound to ruthenium in a  $\eta^6$  fashion, the isopropyl groups on the arene are distorted away from the metal center presumably due to unfavorable steric factors. The two mesityl groups on the IMes ligand are bent towards the ruthenium center with the dihedral angles of  $78.2(2)$  and  $89.9(2)^\circ$  providing steric crowding which appears beneficial in RCM reactions. The allenylidene group is not linear but rather bent at the middle carbon ( $\text{C}22\text{--C}23\text{--C}24 = 171.8^\circ$ ). The  $\text{Ru}\text{--C}22$  ( $1.890(4)$  Å) bond distance is considerably shorter than the  $\text{Ru}\text{--C}(10)$  single bond ( $2.077(4)$  Å).

The catalytic activities of **19**, **20** and **21** have been tested by using the standard ring closing metathesis (RCM) substrate, diethyldiallylmalonate (Scheme 4, reaction 1) and compared to those of  $(p\text{-cymene})\text{RuCl}_2(\text{PR}_3)$  ( $\text{R} = \text{Cy}$  (**22**) and  $i\text{Pr}$  (**23**)). When the reactions were carried out in  $\text{CD}_2\text{Cl}_2$  and heated to  $40^\circ\text{C}$ , **21** catalyzed reaction 1 with a conversion of 85% whereas **19** showed a conversion of 78%. The use of **22** and **23** as catalyst precursors led to the yields of 48 and 47%, respectively, after 27 h (Table 5 entries 1, 2, 5 and 6).

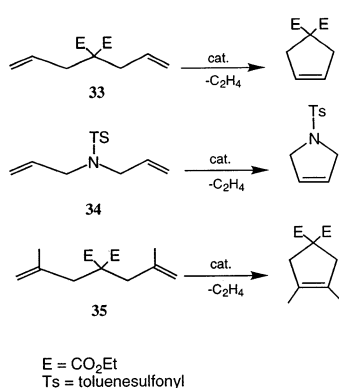
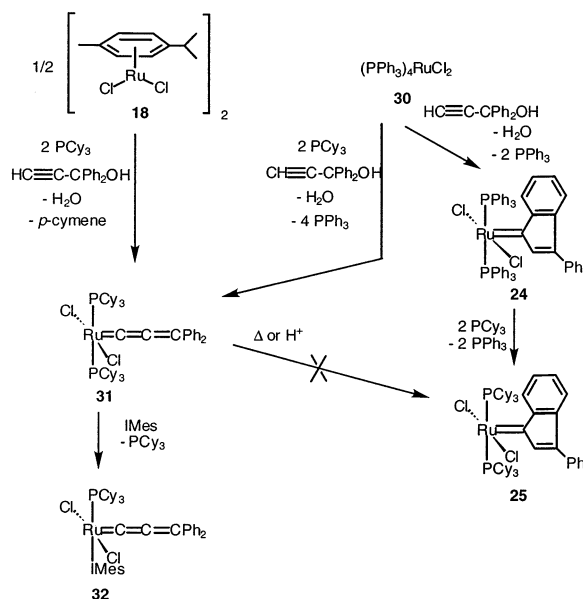
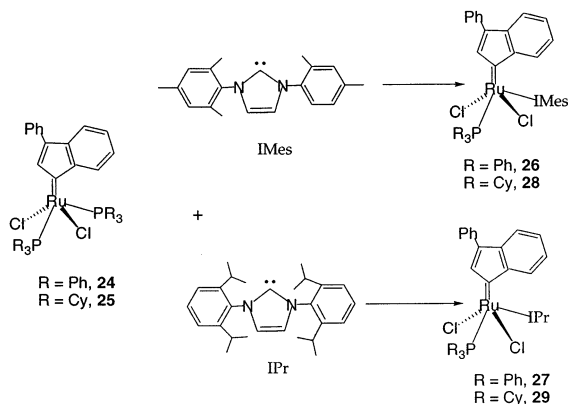
The catalytic activity of **20** at this temperature (40% yield, Table 5 entry 3) was in the range of those of the phosphine containing complexes **22** and **23**. To investigate the role of solvent, temperature and light, RCM was performed with **19** and **20** as the catalyst precursors and  $d_8$ -toluene as the solvent. Upon heating the reaction mixtures to  $80^\circ\text{C}$ , a 100% conversion to product was observed after only 2 h in both cases (Table 5 entries 7 and 9). Performing the reactions in the dark

Table 5  
Ring closing metathesis of diallylmalonate using catalyst precursors **19**, **20**, **21**, **22**, and **23**

Entry	Catalyst precursor	Solvent	Temperature ( $^\circ\text{C}$ )	Time (h)	Conversion (%) <sup>b</sup>
1	<b>21</b>	$\text{CD}_2\text{Cl}_2$	40	27	85
2	<b>19</b>	$\text{CD}_2\text{Cl}_2$	40	27	78
3	<b>20</b>	$\text{CD}_2\text{Cl}_2$	40	27	40
4	<b>20</b> <sup>a</sup>	$\text{CD}_2\text{Cl}_2$	40	27	40
5	<b>22</b>	$\text{CD}_2\text{Cl}_2$	40	27	47
6	<b>23</b>	$\text{CD}_2\text{Cl}_2$	40	27	48
7	<b>19</b>	$d_8$ -toluene	80	2	100
8	<b>19</b> <sup>a</sup>	$d_8$ -toluene	80	2	100
9	<b>20</b>	$d_8$ -toluene	80	2	100

<sup>a</sup> The experiment was performed in absence of light.

<sup>b</sup> Calculated from NMR spectra.



did not change the outcome and yields of the reactions (Table 5 entries 4 and 8) which would indicate that the catalytic reactions are not photo-induced. This is in contrast with the complexes of the type  $M-(p\text{-cymene})Cl_2(PR_3)$  ( $M = Ru, Os$ ;  $R = Cy, ^iPr$ ) which

have been reported to become active ROMP catalysts only when activated by UV irradiation [22]. It has also been reported that RCM in the presence of  $[(p\text{-cymene})(PCy_3)ClRu=C=C=CPh_2]PF_6$  and  $Ru(p\text{-cymene})Cl_2(PCy_3)$  is accelerated by exposure to UV or neon light. [20d,21] No such effect is observed for our system. Complexes **19** and **21** are the best catalyst precursors found in this specific study whereas the ruthenium complex incorporating the IPr ligand, **20**, showed similar reactivity as that displayed by **22** and **23**. From solution calorimetric data, the IMes ligand proved to be a stronger binder than IPr ligand whose relative enthalpy is comparable to that of  $PCy_3$  ligand [10]. The initial step in the ring closing metathesis mechanism using the  $(p\text{-cymene})RuLCl_2$  complexes must involve the formation of a ruthenium–carbene complex [2a,c] and in the case of ruthenium–arene complexes the carbene moiety can presumably be formed by the change in the hapticity of the arene ring, leading to vacant sites on Ru. The more electron donating ligand (IMes) can facilitate this process more easily than either IPr or the phosphines, and this is proposed as the origin of the higher catalytic activity of **19** compared to those of **20**, **22**, and **23** at 40°C. When the temperature is raised to 80°C both **19** and **20** exhibit the same activity. It could be argued that at higher temperatures the activation barrier for the change in arene hapticity has already been overcome and under these conditions the electronic differences between the ligands are not very important.

## 6. Indenylidene–imidazolyliene ruthenium complexes as RCM catalysts

We were also interested in developing the synthesis of imidazol-2-ylidene analogues of the previously synthesized neutral Ru–allenylidene complexes,  $RuCl_2(=C=C=CPh_2)(PR_3)_2$   $R = Ph, Cy$  [20c] via substitution reactions and in comparing their RCM activity to those of the cationic 18-electron ruthenium allenylidene complexes. Analysis of the product of simple substitution reactions showed that the ‘ $C_\alpha$ ’ unsaturated moiety in this complex is not an allenylidene but rather a cyclized vinyl carbene ‘an indenylidene’ (Scheme 2) [23]. An account of the development of this chemistry will be reported in a separate contribution [24].

## 7. 16-Electron ruthenium allenylidene complexes

To develop a method for the synthesis of true neutral ruthenium allenylidene complexes,  $(PPh_3)_4RuCl_2$  (**30**) was allowed to react with 3,3-diphenylpropyn-3-ol in presence of a better donating ligand such as  $PCy_3$  [25] reaction led exclusively to the formation of



(PCy<sub>3</sub>)<sub>2</sub>Ru(=C=C=CPh<sub>2</sub>)Cl<sub>2</sub> (**31**) (see Scheme 3). It is interesting to note that in the absence of PCy<sub>3</sub>, the sole product is the indenylidene complex **24** which undergoes substitution with PCy<sub>3</sub>, to yield **25**. Complex **31** is also accessible from the reaction of [(*p*-cymene)RuCl<sub>2</sub>]<sub>2</sub> **18** with 3,3-diphenylpropyn-3-ol and two equivalents of PCy<sub>3</sub>, via loss of *p*-cymene. However, the product (85% **31** based on <sup>31</sup>P-NMR data) contains two side products, one identified as the 3-phenyl-L-indenylidene complex **25** (8% by NMR data) and one unknown (7% by NMR data). When two equivalents of PPh<sub>3</sub> instead of PCy<sub>3</sub> were used no carbene moiety was formed. All attempts to convert the allenylidene into the indenylidene by addition of protic acids or by subjecting the allenylidene to elevated temperatures were unsuccessful. The exchange of one PCy<sub>3</sub> ligand for IMes affords the allenylidene complex **32** in high yields. These reactions are summarized in Scheme 3. Structural models of **31** and **32** are shown in Figs. 16 and 17, respectively. In both structures the five-coordinated ruthenium center is located at the bottom of a square pyramid. The allenylidene moiety is located at the apex, the trans

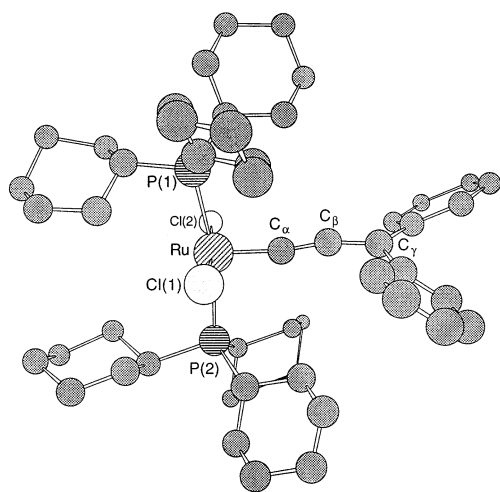


Fig. 16. Molecular structure of (PCy<sub>3</sub>)<sub>2</sub>Ru(=C=C=CPh<sub>2</sub>)Cl<sub>2</sub> (**31**). Hydrogen atoms have been omitted for clarity.

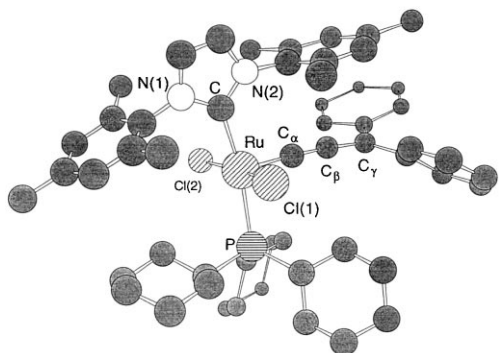


Fig. 17. Molecular structure of (PCy<sub>3</sub>)Ru(IMes)(=C=C=CPh<sub>2</sub>)Cl<sub>2</sub> (**32**). Hydrogen atoms have been omitted for clarity.

chlorides and PCy<sub>3</sub> ligands (**31**), PCy<sub>3</sub> and IMes ligands (**32**), form the base. In both complexes the Ru–Ca bond distances are nearly identical (1.794(11) Å). This is in the usual range (1.761.84 Å) for carbene moieties in these kind of 16-electron ruthenium complexes [10,11]. However, these bond distances are much shorter than the bond lengths determined for cationic 18-electron ruthenium allenylidene complexes (1.871.92 Å) [26]. This indicates a better overlap and a significantly higher bond strength of the carbene moiety to the metal center in complexes **31** and **32**. The comparable metal–ligand bond distances at the base also give very similar values indicating no significant change for the electronic environment of the metal center and these structural features may explain the similar catalytic properties of complexes **31** and **32** (vide infra). The bond angles in both complexes at the base do not deviate more than 4° from ideal 90°. However, steric interference with the allenylidene moiety causes widening of one of each C<sub>α</sub>–Ru–Cl angles (96.2 (5)° (**31**), 95.89(4)° (**32**), one C<sub>α</sub>–Ru–P angle (101.4(5)°) in complex **31** and the C<sub>α</sub>–Ru–C(IMes) angle (98.89(5)°) in complex **32**. The allenylidene chain is only slightly bent in complex **31** (Ru–C<sub>α</sub>–C<sub>β</sub> = 175.36(11)°, C<sub>α</sub>–C<sub>β</sub>–C<sub>γ</sub> = 175.29(13)°). This indicates a strong conjugation along the spine excluding C–H π-interaction to neighboring hydrogen atoms as observed in other complexes. Complex **31**, however, shows significantly stronger bending along the spine (Ru–C<sub>α</sub>–C<sub>β</sub> = 169.20(11)°, C<sub>α</sub>–C<sub>β</sub>–C<sub>γ</sub> = 167.20(18)°). C–H π-interaction to hydrogen atoms of the PCy<sub>3</sub> ligands may be present. This interaction might also have a weak influence on the bond distances along the spine causing a slight extension [C<sub>α</sub>–C<sub>β</sub> = 1.27 Å (**31**), 1.26 Å (**31**) and C<sub>β</sub>–C<sub>γ</sub> = 1.35 Å (**32**), 1.34 Å (**32**)], but these values are in the usual range for ruthenium allenylidene complexes [24].

Solutions containing compounds **31** and **32** were subjected to elevated temperatures. Both compounds were relatively robust at 80°C [23]. Even after 32 h of constant heating no signs of decomposition products were found. Initial signs of decomposition were noticed for complex **31** after 64 h and for complex **32** after 128 h. This goes along with the observed stability trend for the Cl<sub>2</sub>(PCy<sub>3</sub>)(IMes)Ru(=C(H))Ph and Cl<sub>2</sub>(PCy<sub>3</sub>)Ru(=C(H))Ph complexes [10,11].

The role of complexes **31** and **32** as catalyst precursors in the ring closing metathesis (RCM) reactions was investigated with three different diene substrates diethyl diallylmalonate (**33**), diallyltosylamine (**34**) and diethyl di(2-methylallyl)malonate (**35**) [22]. The observed catalytic reactions are depicted in Scheme 4. Both complexes perform very poorly in these reactions compared to the cationic 18-electron arene–ruthenium allenylidene complexes. The significantly higher bond energy of the allenylidene moiety at the metal center as inferred from the single crystal X-ray data may be at the origin of the lower catalytic activity displayed by **31**

and **32**. The sterically hindered substrate diethyl di(2-methylallyl)malonate shows no sign of ring closing using either complexes even after 2 h at 80°C. In order to get detectable conversion of the other substrates, reaction mixtures were heated to 40°C in CD<sub>2</sub>Cl<sub>2</sub>. The turnover rates after 25 min indicated slightly lower catalytic activity for the IMes substituted complex **32** (diethyl diallylmalonate 8%, diallyltosylamine 0%) compared to complex **31** (diethyl diallylmalonate 12%, diallyltosylamine 4%). The disappointingly low catalytic activities for ring closing metathesis reactions obtained for **31** and **32** could be attributed to the very similar metal–carbene bond distances in the solid state indicating a similar electronic environment at the metal center for both complexes.

## 8. Conclusion

The nucleophilic carbenes are ‘phosphine-mimics’ and yet they are much more. They reside at the upper end of the Tolman electronic and steric parameter scales. From solution calorimetric studies, it became clear that nucleophilic carbenes (most of them) are better donors than the best donor phosphines. This stability scale provided by the calorimetry allowed us to propose thermodynamically ‘feasible’ reactions. Developments emerging from our laboratories in this area can be attributed to our initial thermochemistry. Olefin metathesis benefits from the steric protection provided by the nucleophilic carbene fences as well as their electron donating properties.

## Acknowledgements

S.P.N. acknowledges the National Science Foundation (CHE-99085213), the Petroleum Research Fund administered by the ACS and the Louisiana Board of Regents for partial support of this work.

## References

- [1] (a) R.H. Grubbs, *Comprehensive Organometallic Chemistry*, vol. 8, Pergamon, New York, 1982. (b) M. Leconte, J.M. Basset, F. Quignard, C. Larroche, *Reactions of Coordinated Ligands*, vol. 1, Plenum, New York, 1986. (c) J. Feldman, R.R. Schrock, *Progress in Inorganic Chemistry*, vol. 39, Wiley, New York, 1991. (d) K.J. Ivin, J.C. Mol, *Olefin Metathesis and Metathesis Polymerization*, Academic Press, San Diego, 1997. (e) J.C. Mol, J.A. Moulijn, *Catalysis: Science and Technology*, vol. 8, Springer Verlag, Berlin, 1987. (f) R.H. Grubbs, S.J. Miller, G.C. Fu, *Acc. Chem. Res.* 28 (1995) 446.
- [2] (a) P. Schwab, M.B. France, J.W. Ziller, R.H. Grubbs, *Angew. Chem. Int. Ed. Engl.* 34 (1995) 2039. (b) P. Schwab, R.H. Grubbs, J.W. Ziller, *J. Am. Chem. Soc.* 118 (1996) 100. (c) E.L. Diaz, S.T. Nguyen, R.H. Grubbs, *J. Am. Chem. Soc.* 119 (1997) 3887 and references cited therein.
- [3] R.R. Schrock, J.S. Mursdek, G.C. Bazan, J. Robbins, M. DiMare, M. O'Regan, *J. Am. Chem. Soc.* 112 (1990) 3875.
- [4] (a) S.T. Nguyen, R.H. Grubbs, J.W. Ziller, *J. Am. Chem. Soc.* 115 (1993) 9858. (b) S.T. Nguyen, L.K. Johnson, R.H. Grubbs, *J. Am. Chem. Soc.* 114 (1992) 3974. (c) A.W. Stumpf, E. Saive, A. Demonceau, A.F. Noels, *J. Chem. Soc. Chem. Commun.* (1995) 1127. (d) Z. Wu, S.T. Nguyen, R.H. Grubbs, J.W. Ziller, *J. Am. Chem. Soc.* 117 (1995) 5503. (e) W.A. Herrmann, W.C. Schattermann, O. Nuyken, S.C. Glander, *Angew. Chem. Int. Ed. Engl.* 35 (1996) 1087. (f) B. Mohr, D.M. Lynn, R.H. Grubbs, *Organometallics* 15 (1996) 4317. (g) A. Demonceau, A.W. Stumpf, E. Saive, A.F. Noels, *Macromolecules* 30 (1997) 3127. (h) J.S. Kingsbury, J.P.A. Harrity, P.J. Bonitatebus Jr., A.H. Hoveyda, *J. Am. Chem. Soc.* 121 (1999) 791. (i) A. Fürstner, O.R. Thiel, L. Ackerman, H.-J. Schanz, S.P. Nolan, *J. Org. Chem.* 65 (2000) 2204.
- [5] M. Ulman, R.H. Grubbs, *J. Org. Chem.* 64 (1999) 7202.
- [6] (a) W.A. Herrmann, C. Kocher, *Angew. Chem. Int. Ed. Engl.* 36 (1997) 2162. (b) A.J. Arduengo, *Acc. Chem. Res.* 32 (1999) 913. (c) D. Bourissou, O. Guerret, F. Gabbai, G. Bertrand, *Chem. Rev.* 100 (2000) 39. (d) A.J. Arduengo III, H.V. Rasika Dias, R.L. Harlow, M. Kline, *J. Am. Chem. Soc.* 114 (1992) 5530. (e) H. Wanzlick, *Angew. Chem. Int. Ed. Engl.* 1 (1962) 75. (f) M.F. Lappert, *J. Organomet. Chem.* 358 (1988) 185. (g) A.J. Arduengo III, R. Krafczyk, *Chem. In Unserer Zeit.* 32 (1998) 6.
- [7] J. Huang, H.-J. Schanz, E.D. Stevens, S.P. Nolan, *Organometallics* 18 (1999) 2370.
- [8] B.K. Campion, R.H. Heyn, T.D. Tilley, *Chem. Commun.* (1988) 278.
- [9] S.A. Serron, J. Huang, S.P. Nolan, *Organometallics* 17 (1998) 534.
- [10] J. Huang, E.D. Stevens, S.P. Nolan, J.L. Petersen, *J. Am. Chem. Soc.* 121 (1999) 2674.
- [11] L. Jafarpour, E.D. Stevens, S.P. Nolan, *J. Organomet. Chem.* 606 (2000) 49.
- [12] L.H. Pignolet, *Homogeneous Catalysis with Metal Phosphine Complexes*, Plenum, New York, 1983.
- [13] C.A. Tolman, *Chem. Rev.* 77 (1977) 313.
- [14] (a) T. Weskamp, W.C. Schattenmann, M. Spiegler, W.A. Herrmann, *Angew. Chem. Int. Ed. Engl.* 37 (1998) 2490. (b) T. Weskamp, K.J. Kohl, W. Hieringer, D. Gleich, W.A. Herrmann, *Angew. Chem. Int. Ed. Engl.* 38 (1999) 2416. (c) M. Scholl, T.M. Trnka, J.P. Morgan, R.H. Grubbs, *Tetrahedron Lett.* 40 (1999) 2247.
- [15] G.J. Kubas, *Acc. Chem. Res.* 21 (1988) 120.
- [16] J. Huang, H.-J. Schanz, E.D. Stevens, S.P. Nolan, *Organometallics* 18 (1999) 5375.
- [17] L. Jafarpour, S.P. Nolan, *Organometallics* 19 (2000) 2055.
- [18] (a) M. Scholl, S. Ding, C.W. Lee, R.H. Grubbs, *Org. Lett.* 1 (1999) 953. (b) A.K. Chatterjee, J.P. Morgan, M. Scholl, R.H. Grubbs, *J. Am. Chem. Soc.* 122 (2000) 3783.
- [19] A.K. Chatterjee, J.P. Morgan, M. Scholl, R.H. Grubbs, *J. Am. Chem. Soc.* 122 (2000) 3783.
- [20] (a) A. Fürstner, M. Picquet, C. Bruneau, P.H. Dixneuf, *Chem. Commun.* (1998) 1315. (b) A. Fürstner, L. Ackermann, *Chem. Commun.* (1999) 95. (c) K.J. Harlow, A.F. Hill, J.D.E.T. Wilton-Ely, *J. Chem. Soc. Dalton Trans.* (1999) 285. (d) A. Fürstner, A.F. Hill, M. Liebl, J.D.E.T. Wilton-Ely, *Chem. Commun.* (1999) 601. (e) L. Jafarpour, J. Huang, E.D. Stevens, S.P. Nolan, *Organometallics* 18 (1999) 3760.
- [21] M. Picquet, C. Bruneau, P.H. Dixneuf, *Chem. Commun.* (1998) 2249.

- [22] A. Hafner, A. Mühlebach, P.A. van der Schaaf, *Angew. Chem. Int. Ed. Engl.* 36 (1997) 2121.
- [23] L. Jafarpour, H.-J. Schanz, E.D. Stevens, S.P. Nolan, *Organometallics* 18 (1999) 5416.
- [24] A.F. Hill, A. Fürstner, L. Jafarpour, S.P. Nolan, manuscript in preparation.
- [25] H.-J. Schanz, L. Jafarpour, E.D. Stevens, S.P. Nolan, *Organometallics* 18 (1999) 5187.
- [26] (a) J. Selegue, *Organometallics* 1 (1982) 217. (b) M.P. Gamasa, J. Gimeno, C. Gonzalez-Bernardo, J. Borge, S. Garcia-Granada, *Organometallics* 16 (1997) 2483. (c) B. Buriez, I.D. Burns, A.F. Hill, A.J.P. White, P.J. Williams, J.D.E.T. Wilton-Ely, *Organometallics* 18 (1999) 1504. (d) V. Cadierno, M.P. Gamasa, J. Gimeno, L. Iglesias, S. Garcia-Granada, *Inorg. Chem.* 38 (1999) 2874.